

Scenario-based Measurement of Interest Rate Risks*

Sebastian Schlütter[†]

This version: 28th October 2020

Abstract

Principal component analysis (PCA) is an important method for measuring interest rate risks on the basis of stress scenarios of future yield curves. The aggregation of portfolio losses resulting from stressed yield curves typically takes place using a square-root formula. This paper explores how accurately a scenario-based approach can reflect interest rate risks in comparison with a stochastic model. To this end, we simulate future yield curves using a stochastic version of the Nelson-Siegel model. Afterwards, we employ a PCA to translate the simulated yield curves into stress scenarios. For a large number of randomly generated asset-liability portfolios, we determine the Value-at-Risk (VaR) based on the stochastic model and based on the stress scenarios. We find that the approximation error from using stress scenarios instead of the complete stochastic model can be substantially reduced by incorporating VaR-implied tail correlation parameters into the square-root formula. This method of improvement is straightforward with the replacement of Pearson correlations by VaR-implied tail-correlations in situations where risk factors are not elliptically distributed.

Keywords: Value-at-Risk, Interest Rate Risk, Principal Component Analysis, Solvency II

JEL classification: G17, G22, G28

*A former version of this paper was titled “Scenario-Based Capital Requirements for the Interest Rate Risk of Insurance Companies”. The author is grateful for helpful comments from the participants of the Annual Congress of the German Association for Insurance Sciences (2017), the Workshop on “Financial Management & Financial Institutions” (2017) of the German Operations Research Society, the Research Seminar of Deutsche Bundesbank, the Annual Meeting of the Asia-Pacific Risk and Insurance Association (2017), the Annual Meeting of the American Risk and Insurance Association (2017), the CEQURA Conference on Advances in Financial and Insurance Risk Management (2017), the Annual Meeting of the German Finance Association (2017) as well as the International Congress of Actuaries (2018). Grateful acknowledgement is also given to Deutsche Bundesbank as well as to the Hagen Family Foundation for financially supporting conference attendances for the presentation of this paper.

[†]Mainz University of Applied Sciences, School of Business, Lucy-Hillebrand-Str. 2, 55128 Mainz, Germany; Fellow of the International Center for Insurance Regulation, Goethe University Frankfurt; email: sebastian.schluetter@hs-mainz.de.

1 Introduction

Many regulatory approaches employ stress scenarios of future yield curves for measuring interest rate risks of financial institutions. The Solvency II standard formula, which is applied by most insurance companies in the European Union, employs stress scenarios reflecting upward or downward movements of the yield curve.¹ Insurers have to reevaluate their assets and liabilities with regard to these two scenarios; the capital requirement for interest rate risks is the loss in equity capital in the worse of the two scenarios. Similarly, interest rate risks are measured based on stressed yield curves in the Chinese insurance regulation system (Fung et al., 2018, p. 21). The International Capital Standard considers multiple stress scenarios, including changes in the level, slope and curvature of the yield curve International Association of Insurance Supervisors (IAIS) (2020, pp. 55 ff.). To assess the interest rate risks to which banks are exposed in their banking book, Bank for International Settlements (2016, p. 44 ff.) defines six stress scenarios of the yield curve which banks should use as a basis for calculating the impact on their economic value and their earnings. In the context of identifying outlier banks, the maximal loss in capital according to six prescribed scenarios is relevant.² In addition, banks are supposed to consider internally selected scenarios which address their specific risk profile.³

The literature typically applies stochastic models for measuring interest rate risks. Many papers apply affine factor models, such as the models of Cox et al. (1985) or Vasicek (1977). These models have been adapted into a life insurance context by Gerstner et al.

¹In the current regulation, stress scenarios are defined by factors which are multiplied with current interest rates, cf. European Commission (2015), Articles 166 f. In terms of the 2020 review of Solvency II, the procedure may change in such a manner that additive as well as multiplicative stress parameters are in place, cf. European Insurance and Occupational Pensions Authority (EIOPA) (2019, p. 352 ff.).

²Cf. Bank for International Settlements (2016), p. 25.

³Cf. Bank for International Settlements (2016), p. 25.

(2008) and Graf et al. (2011), for example. Another starting point for a stochastic interest rate model is offered by the model of Nelson and Siegel (1987), which uses three factors to govern the level, slope and curvature of the yield curve. Diebold and Li (2006) derive good forecasts of future yield curves by modeling the development of the three factors over time with stochastic processes. Caldeira et al. (2015) estimate the Value-at-Risk (VaR) of fixed income portfolios over a 1-day holding period based on the factor models of Nelson and Siegel (1987) and Svensson (1994). Caldeira et al. model the development of the factor scores over time using vector-autoregressive (VAR) processes. The disturbances of this VAR process are modeled using the dynamic conditional correlation (DCC) model as proposed by Engle (2002). The authors demonstrate the accuracy of their VaR estimates by backtesting them against historical yield curve movements.

Another strand of literature demonstrates that the simple deterministic interest rate risk measurement employed by regulatory capital requirements often provides a biased assessment. Gatzert and Martin (2012) compare the outcomes of the Solvency II standard formula with the corresponding results of a stochastic model for equity, interest rate and credit risks. The authors find that the standard formula can overstate or understate the risk depending on the composition of the portfolio, for example because it improperly accounts for diversification effects. Martin (2013) finds that the standard formula provides similar outcomes to the model of Vasicek (1977), whereas the model of Cox et al. (1985) leads to a lower capital requirement. Moreover, Laas and Siegel (2017) identify inconsistencies in the interest rate risk measurement between Solvency II and Basel III. Braun et al. (2017) show that an improperly calibrated market risk model in the Solvency II standard formula can induce insurers to select an inefficient portfolio in the sense of

Markowitz portfolio optimization. As a consequence, firms can attain an increased default risk level (cf. also Fischer and Schlütter, 2014).

This paper studies how appropriately a scenario-based approach can measure interest rate risks. In line with Diebold and Li (2006) and Caldeira et al. (2015), our analysis starts from a dynamic version of the Nelson and Siegel (1987) model (DNS model).⁴ In line with Caldeira et al. (2015), we employ VAR processes for the development of the DNS model’s factor scores over time and model their disturbances using Engle’s DCC model. The DNS model, as considered by Caldeira et al. (2015), does not account for lower bounds for interest rates and could hence simulate high negative interest rates, which are not reasonable from an economic perspective. To address this issue, we propose another variant of the stochastic interest rate process by using the DNS model for the logarithmic difference between interest rates and their lower bounds.⁵ We call this variant of the model the “Log-DNS” model. Each of these models, the original DNS model and the Log-DNS model, describes how the yield curve and hence the value of an asset-liability portfolio evolves over time. On this basis, we determine a portfolio’s VaR.

To determine a portfolio’s VaR approximately based on stress scenarios, we employ a principal component analysis (PCA) in line with Frye (1997), Golub and Tilman (1997) and Hull (2018, pp. 535 ff.). With respect to each of the most relevant principal com-

⁴According to Diebold and Li (2006), the yield curve forecasts based on the DNS model outperform those of affine factor models, which we therefore do not use. The weak performance of affine factor models in forecasting the yield curve has also been highlighted by Duffee (2002). Moreover, by modeling the short rate, affine factor models focus on yield curve shifts and may therefore understate the risk of changes in the steepness or the curvature of the yield curve. Vedani et al. (2017) point out that an insurance-specific version of the LIBOR Market Model, which is often employed by practitioners to value options and guarantees embedded in insurance liabilities, leads to spurious simulated yield curves when the model is applied for longer time horizons.

⁵An alternative approach for incorporating lower bounds for interest rates has been proposed by Eder et al. (2014). The authors include lower bounds by means of a plane-truncated normal distribution. However, the approach is numerically extensive, and it therefore seems difficult to combine it with a GARCH process to address heteroscedasticity in longer time horizons.

ponents, a portfolio loss relating to the stressed yield curve is calculated. The aggregate VaR of the portfolio is the square-root of the sum of the squared losses. We show that this procedure is precise if the discount factors follow a multivariate elliptical distribution. For multivariate elliptical distributions, the square-root formula in connection with Pearson correlations allows for an accurate risk aggregation (McNeil et al., 2015, pp. 295), and by construction, the principal component scores are uncorrelated. Given that the stochastic models employed do not provide elliptically distributed discount factors, we propose including a small number of VaR-implied correlations, as proposed by Campbell et al. (2002) and Mittnik (2014), when aggregating the scenario outcomes.

We backtest the VaR estimates based on the complete stochastic model and based on the stress scenarios against historical yield curve changes. To this end, we consider 1,000 hypothetical asset-liability portfolios and various combinations of confidence levels and holding periods. For each portfolio, the accuracy of the VaR is measured by the portion of historical time windows for which the VaR is lower than the loss in value that the portfolio experienced for the actual change in interest rates (hit rate). The backtesting results demonstrate that the accuracy of the VaR estimates provided by the Log-DNS model is similar to those of the DNS model. Hence, the Log-DNS model's advantage of complying with a lower bound for interest rates is not dampened by deficiencies in terms of the accuracy. Moreover, we find that the VaR according to both DNS and Log-DNS models is suitable for most of the asset-liability portfolios considered, i.e. not only for an equally-weighted asset portfolio as considered by Caldeira et al. (2015). Our backtesting results for the scenario-based assessment demonstrate that a calculation based on four scenarios (corresponding to two principal components) in connection with two correlation parameters provides a close approximation of simulation-based VaR.

The remainder of the paper is organized as follows. Section 2 outlines the methodology for stochastically modeling interest rate risk, determining the Value-at-Risk and transforming the simulated yield curves into a scenario-based calculation for the Value-at-Risk. Section 3 calibrates the models based on yield curve data published by the European Central Bank (ECB). Section 4 provides the backtesting of the stochastic models as well as of the scenario-based approximation. Section 5 concludes.

2 Value-at-Risk of interest rate risks

2.1 Stochastic model of interest rate risks

Our starting point for modeling interest rates is the dynamic version of the model from Nelson and Siegel (1987), as proposed by Diebold and Li (2006) and employed for the calculation of Value-at-Risk by Caldeira et al. (2015). Let $M \in \mathbb{N}$ denote the largest maturity under consideration. We assume that the continuously compounded interest rates for a set of maturities $\{\tau_1, \dots, \tau_m\} \subset \{1, \dots, M\}$ are described by an m -dimensional stochastic process in discrete time.⁶ At time $t \in \mathbb{N}_0$, interest rates are defined by

$$r_t = \begin{pmatrix} r_t(\tau_1) \\ \vdots \\ r_t(\tau_m) \end{pmatrix} = \Lambda(\lambda, \tau_1, \dots, \tau_m) f_t + \epsilon_t, \quad (1)$$

where $\Lambda(\lambda, \tau_1, \dots, \tau_m)$ is a $m \times 3$ matrix of factor loadings, f_t is a 3-dimensional stochastic process of factor scores and ϵ_t is an m -dimensional stochastic process of disturbances.

⁶In our calibrations in section 3, we consider how yield curves evolve in terms of trading days.

According to Diebold and Li (2006, p. 341), each row $i \in \{1, \dots, m\}$ of the matrix of factor loadings $\Lambda(\lambda, \tau_1, \dots, \tau_m)$ is defined as

$$\left[1, \frac{1 - e^{-\tau_i/\lambda}}{\tau_i/\lambda}, \frac{1 - e^{-\tau_i/\lambda}}{\tau_i/\lambda} - e^{-\tau_i/\lambda} \right] \quad (2)$$

The components of the vector of factors scores $f_t = (\beta_{1,t}, \beta_{2,t}, \beta_{3,t})^T$ can be intuitively interpreted:⁷ $\beta_{1,t}$ reflects the long-term level of the yield curve, since its loading is constantly 1. The loading on $\beta_{2,t}$ starts at 1 if τ_i is close to zero and decreases to zero if τ_i becomes large. Hence, $\beta_{2,t}$ can be viewed as the short-term interest rate, and it governs the slope of the yield curve. The loading on $\beta_{3,t}$ starts at zero, becomes positive and finally converges to zero if τ_i moves from 0 to infinity. Hence, $\beta_{3,t}$ steers medium-term interest rates, or the curvature of the yield curve.

In order to avoid the modeled interest rates falling below an economically reasonable level, we consider an additional specification of the model, which incorporates a lower bound for interest rates. The right-hand side of Eq. 1 is now used to model the logarithmic difference between the interest rate and a lower bound for the interest rate:

$$\ln(r_t - r^{min}) = \Lambda(\lambda, \tau_1, \dots, \tau_m) f_t + \epsilon_t, \quad (3)$$

where $r^{min} = (r^{min}(\tau_1), \dots, r^{min}(\tau_m))^T$ is the vector of lower bounds per maturity τ_i , the logarithm is applied to every entry of the vector $(r_t - r^{min})$ separately, and $\Lambda(\lambda, \tau_1, \dots, \tau_m)$ is defined as in Eq. 2. As for the model in Eq. 1, the factor scores $f_t = (\beta_{1,t}, \beta_{2,t}, \beta_{3,t})^T$

⁷Cf. Diebold and Li (2006, p. 341 f.).

govern the level, slope and curvature of the yield curve. We refer to this model as the Log-DNS model.

For the DNS and Log-DNS models, the development of the parameter vector f_t over time may exhibit autocorrelation. We address autocorrelation by a vector-autoregressive (VAR) model, in which the development of each entry f_t depends on the history of all entries of f_t :⁸

$$\Delta f_t = \mu + \sum_{k=1}^p \Gamma_k \cdot f_{t-k} + \eta_t, \quad (4)$$

where $\Delta f_t = f_t - f_{t-1}$, $p \in \mathbb{N}$ is the lag order of the VAR process, $\mu \in \mathbb{R}^3$ is a vector of constant coefficients, Γ_k are 3×3 transition matrices, and the 3-dimensional stochastic process η_t reflects the disturbances.

The disturbances process η_t may exhibit time-varying volatilities and correlations. The backtesting results of Caldeira et al. (2015, p. 77-79) indicate that the dynamic conditional correlation (DCC) model proposed by Engle (2002) is appropriate to model the disturbances. In this model, the covariance matrix Ω_t is decomposed into a time-varying correlation matrix R_t and a 3×3 diagonal matrix D_t such that

$$\Omega_t = D_t R_t D_t. \quad (5)$$

Using

$$z_t = D_t^{-1} \eta_t, \quad (6)$$

⁸As an alternative to the VAR model, one could describe the development of each entry of f_t separately using an autoregressive (AR) model. Since the backtesting results of Caldeira et al. (2015, p. 77-79) demonstrate that the VAR model works better than a combination of AR models, we omit the latter specification.

the η_t are transformed into (3×1) -vectors z_t of uncorrelated, standardized disturbances with mean zero and variance one. The elements in the correlation matrices R_t are denoted by $\rho_{i,j,t}$ and obtained as

$$\rho_{i,j,t} = \frac{q_{i,j,t}}{\sqrt{q_{i,i,t}q_{j,j,t}}}, \quad (7)$$

where the $q_{i,j,t}$ are the elements of 3×3 matrices Q_t . The diagonal matrix D_t and the matrix Q_t follow GARCH-like processes:

$$D_t^2 = \text{diag}(\omega_i) + \text{diag}(\kappa_i) \circ \eta_{t-1}\eta_{t-1}^T + \text{diag}(\lambda_i) \circ D_{t-1}^2 \quad (8)$$

$$Q_t = (1 - a - b)\bar{Q} + az_{t-1}z_{t-1}^T + bQ_{t-1} \quad (9)$$

where $\text{diag}(x_i)$ generates a 3×3 diagonal matrix with x_1, x_2, x_3 on the diagonal, \circ denotes the Hadamard product, \bar{Q} is the unconditional covariance matrix, $\omega_i, \kappa_i, \lambda_i$ are non-negative parameters for all $i \in \{1, 2, 3\}$, and a, b are non-negative parameters such that $a + b < 1$.

Finally, the residuals ϵ_t of the DNS and Log-DNS models may exhibit autocorrelation. We address this by modeling the residuals for maturities τ_1, \dots, τ_m by means of autoregressive processes with lag order 1. The disturbances of these AR(1) processes are modeled by independent normal distributions. At time $t = 0$, the processes f_t and ϵ_t start at deterministic vectors and hence, r_0 is a deterministic vector.

In total, both models can be used to simulate interest rates at a future point in time for all maturities of interest, $\tau \in \{1, \dots, M\}$. To extrapolate the simulated interest rates for maturities τ_1, \dots, τ_m towards interest rates for all maturities $1, \dots, M$, the model of Svensson (1994) is used. The Svensson model is regularly employed by central banks to

elicit a yield curve out of bond market data.⁹ It extends the Nelson-Siegel model by an additional factor and determines interest rates as $r_t(\tau) = \Lambda(\lambda_1, \lambda_2, \tau_1, \dots, \tau_M)f_t$, where each row $i \in \{1, \dots, M\}$ of the matrix of factor loadings $\Lambda(\lambda_1, \lambda_2, \tau_1, \dots, \tau_M)$ is defined as

$$\left[1, \frac{1 - e^{-\tau_i/\lambda_1}}{\tau_i/\lambda_1}, \frac{1 - e^{-\tau_i/\lambda_1}}{\tau_i/\lambda_1} - e^{-\tau_i/\lambda_1}, \frac{1 - e^{-\tau_i/\lambda_2}}{\tau_i/\lambda_2} - e^{-\tau_i/\lambda_2} \right] \quad (10)$$

Using the Svensson model for the extrapolation allows us to model the residuals ϵ_t only for a small set of maturities $\{\tau_1, \dots, \tau_m\}$ and receive a meaningful yield curve for every simulation path of the stochastic model.

2.2 Value-at-Risk based on the stochastic model

We consider a portfolio providing deterministic cash flows $S_\tau \in \mathbb{R}$ at the future points in time $\tau \in \{1, \dots, M\}$. The cash flows are collected in a column vector $S = (S_1, \dots, S_M)^T$. We determine the portfolio's Value-at-Risk with regard to the loss in portfolio value due to an instantaneous change in interest rates.¹⁰ The portfolio's Value-at-Risk with confidence level $1 - \alpha$ and holding period h is obtained as

$$\text{VaR}_{1-\alpha, h} = -q_\alpha \left(\sum_{\tau=1}^M e^{-\tau \cdot r_h(\tau)} S_\tau - \sum_{\tau=1}^M e^{-\tau \cdot r_0(\tau)} S_\tau \right), \quad (11)$$

where $q_\alpha(X)$ denotes the α -quantile of the random variable X .

⁹For instance, the yield data used for the calibration later on in section 3.1 have been obtained by the European Central Bank (ECB) based on the Svensson model.

¹⁰Hence, we assume that the length of the time period until the cash flows realize is fixed when the yield curve evolves up to the holding period of the VaR. This view is consistent with Solvency II regulations, cf. European Commission (2015), articles 166 f.

2.3 Scenario-based Value-at-Risk

This section explains how to derive stressed yield curves from a PCA and how to derive a portfolio's Value-at-Risk based on scenarios. Consider a portfolio with cash flows $(S_{\tau_1}, \dots, S_{\tau_m})^T$ occurring at the maturities from section 2.1. Let X_t denote the random vector with the discount factors corresponding to interest rates for those maturities at time $t \geq 0$:

$$X_t = \left(e^{-\tau_1 \cdot r_t(\tau_1)}, \dots, e^{-\tau_m \cdot r_t(\tau_m)} \right)^T \quad (12)$$

Then, the portfolio's Value-at-Risk can be determined by

$$\text{VaR}_{1-\alpha, h} = -\left(q_\alpha(X_h^T \cdot S) - X_0^T \cdot S \right) \quad (13)$$

In order to reduce the required information for this calculation, we transform X_h into its principal components. Let the matrix $\Theta \in \mathbb{R}^{m \times m}$ include the eigenvectors of the covariance matrix of X_h (corresponding to eigenvalues ordered from large to small). We can construct

$$\begin{aligned} Y &= \Theta^{-1} \cdot (X_h - \mathbb{E}[X_h]) \\ \Leftrightarrow X_h &= \Theta \cdot Y + \mathbb{E}[X_h] \end{aligned} \quad (14)$$

The m -dimensional random vector Y satisfies $\mathbb{E}[Y] = 0$ and its covariance matrix is a diagonal matrix. We can recalculate the Value-at-Risk in line (13) as

$$\begin{aligned}
\text{VaR}_{1-\alpha, h} &= -(q_\alpha((\Theta \cdot Y + \mathbb{E}[X_h])^\top \cdot S) - X_0^\top \cdot S) \\
&= -q_\alpha((\Theta \cdot Y)^\top \cdot S) - (\mathbb{E}[X_h] - X_0)^\top \cdot S \\
&= -q_\alpha\left(\sum_{i=1}^m Y_i \cdot (\Theta^\top \cdot S)_i\right) - (\mathbb{E}[X_h] - X_0)^\top \cdot S
\end{aligned} \tag{15}$$

Here, $(\Theta^\top \cdot S)_i$ is the i -th entry of the vector $(\Theta^\top \cdot S)$ and reflects the insurer's exposure to the i -th principal component. Let us assume for a moment that X_h (and hence Y) follow a multivariate elliptical distribution, and let us denote the α -percentile of the standardized marginal distribution by z_α . Then, the Value-at-Risk in line 15 can be determined by

$$\sqrt{\text{var}\left(\sum_{i=1}^m Y_i \cdot (\Theta^\top \cdot S)_i\right)} \cdot z_\alpha - (\mathbb{E}[X_h] - X_0)^\top \cdot S, \tag{16}$$

where $\text{var}(X)$ denotes the variance of X . Since the covariance matrix of Y is diagonal, line (16) can be rewritten as

$$\sqrt{\sum_{i=1}^m \text{var}(Y_i) \cdot (\Theta^\top \cdot S)_i^2} \cdot z_\alpha - (\mathbb{E}[X_h] - X_0)^\top \cdot S \tag{17}$$

According to the assumption of an elliptical distribution, we have

$$\text{var}(Y_i) \cdot (\Theta^\top \cdot S)_i^2 \cdot z_\alpha^2 = \underbrace{\left(q_\alpha(Y_i \cdot (\Theta^\top \cdot S)_i)\right)}_{\text{VaR}_i}^2 \tag{18}$$

The quantile on the right-hand side of Eq. 18 measures the risk related to principal component i , which we denote by VaR_i . Irrespective of the distribution assumption for Y , we can rewrite VaR_i by pulling out the factor $(\Theta^T \cdot S)_i$:

$$\begin{aligned} \text{VaR}_i &= \begin{cases} q_\alpha(Y_i) \cdot (\Theta^T \cdot S)_i & \text{if } (\Theta^T \cdot S)_i \geq 0 \\ q_{1-\alpha}(Y_i) \cdot (\Theta^T \cdot S)_i & \text{if } (\Theta^T \cdot S)_i < 0 \end{cases} \\ &= \begin{cases} \sum_{j=1}^m (X_{0,j} + q_\alpha(Y_i) \cdot \Theta_{j,i}) \cdot S_j - X_0 \cdot S & \text{if } (\Theta^T \cdot S)_i \geq 0 \\ \sum_{j=1}^m (X_{0,j} + q_{1-\alpha}(Y_i) \cdot \Theta_{j,i}) \cdot S_j - X_0 \cdot S & \text{if } (\Theta^T \cdot S)_i < 0 \end{cases} \end{aligned} \quad (19)$$

where $X_{0,j} = e^{-\tau_j \cdot r_0(\tau_j)}$ denotes the j -th element of X_0 . The expressions $X_{0,j} + q_\alpha(Y_i) \cdot \Theta_{j,i}$ and $X_{0,j} + q_{1-\alpha}(Y_i) \cdot \Theta_{j,i}$ in line 19 can be comprehended as discount factors for maturity τ_j years and related to principal component i . For each principal component i , the discount factors can be translated into “stressed” yield curves:

$$r^{i,1}(\tau) = -\ln[X_{0,j} + q_\alpha(Y_i) \cdot \Theta_{j,i}] / \tau_j \quad (20)$$

and

$$r^{i,2}(\tau) = -\ln[X_{0,j} + q_{1-\alpha}(Y_i) \cdot \Theta_{j,i}] / \tau_j, \quad (21)$$

with $j = 1, \dots, m$. Hence, the Value-at-Risk related to principal component i is calculated as the change in portfolio value when the yield curve changes in a stress scenario.

In order to receive the Value-at-Risk for interest rate risk in total, the results for VaR_i are aggregated as in Eq. 17. Since the first few components typically explain a large share of

the variation, a good approximation of the Value-at-Risk might already be achieved by taking only the first $\tilde{m} < m$ components into account:

$$\text{VaR}_{1-\alpha,h} \approx \sqrt{\sum_{i=1}^{\tilde{m}} \text{VaR}_i^2} - (\mathbb{E}[X_h] - X_0)^T \cdot S \quad (22)$$

An appropriate value for \tilde{m} needs to trade off the benefits of a higher accuracy against the costs of a more complex calculation, since more scenarios need to be evaluated.

2.4 Scenario-based Value-at-Risk with correlation parameters

As an alternative to increasing the number of scenarios, there is a more effective possibility for improving the accuracy of the scenario-based Value-at-Risk. When aggregating the Value-at-Risks relating to the principal components, Eq. 22 does not make use of correlations, since the scores of principal components are by definition uncorrelated. A natural generalization of Eq. 22 is to allow for correlations when aggregating the Value-at-Risks VaR_k :

$$\text{VaR}_{1-\alpha,h} \approx \sqrt{\sum_{i=1}^{\tilde{m}} \sum_{j=1}^{\tilde{m}} \rho_{i,j} \cdot \text{VaR}_i \cdot \text{VaR}_j} - (\mathbb{E}[X_h] - X_0)^T \cdot S \quad (23)$$

with $\rho_{i,i} = 1$ for all $i = 1, \dots, \tilde{m}$. Campbell et al. (2002) suggest estimating the parameters $\rho_{i,j}$ implicitly, such that they imply an optimal fit between the aggregation based on the square-root formula and the portfolio's Value-at-Risk in accordance with the true multivariate distribution. In the aggregation of risk (sub-)modules in the Solvency-II-standard formula, the correlation parameters “should be chosen in such a way as to achieve the best approximation of the 99.5% VaR for the aggregated capital requirement”, reflect-

ing imperfections with this aggregation formula such as skewed distributions.¹¹ Hence, even though the Pearson correlation between the principal component scores is zero, correlation parameters may be included in Eq. 23 to outweigh deficiencies resulting from skewed or fat-tailed distributions of the principal component scores, thereby improving the accuracy of the approximation.

Mitnik (2014) suggests identifying the correlation parameters that ensure an optimal fit of Eq. 23 simultaneously for various calibration portfolios. Transferring this idea to our context means that the correlation parameters should minimize

$$\sum_{i=1}^N \left(\widehat{\text{VaR}}(i) - \text{VaR}(i) \right)^2 \quad (24)$$

where $\widehat{\text{VaR}}(i)$ is the approximate Value-at-Risk for calibration portfolio i according to the right-hand side of Eq. 23, $\text{VaR}(i)$ is the Value-at-Risk according to the interest-rate model from section 2.1 and N is the number of calibration portfolios. According to Mitnik (2014), the calibration portfolios should reflect practical considerations and account, for example, for asset allocation limits.

3 Calibration of interest rate models

3.1 Data

The model calibration is based on data published by the ECB, which estimates the yield curve from AAA-rated Euro-area central government bonds with the Svensson model.¹²

¹¹The verbatim quote is from CEIOPS (2010, p. 339).

¹²Cf. <https://www.ecb.europa.eu/stats/money/yc/html/index.en.html>

The ECB has published the 6 parameters of the Svensson model, together with the corresponding interest rates for maturities 1, 5, 10, 20 and 30 years for every trading day since 6 September 2004. We use these data on a daily basis from 6 September 2004 to 30 December 2019, giving us 3917 observations of the yield curve. Table 1 shows the descriptive statistics for the daily changes in interest rates for maturities 1, 5, 10, 20 and 30 years.

Table 1: Descriptive statistics for daily changes in interest rates from 6.9.2004 to 30.12.2019 (in basis points).

Maturity	Mean	Std Dev.	Min	Max	Skewness	Kurtosis
1	-0.076	2.401	-26.368	19.440	-0.728	16.235
5	-0.100	3.647	-22.579	18.312	0.028	5.522
10	-0.111	3.728	-19.305	18.054	0.168	4.693
20	-0.116	4.087	-24.100	24.027	0.055	5.938
30	-0.118	4.680	-56.403	31.075	-0.267	11.568

3.2 Calibration

When calibrating the Log-DNS model, we set $r^{min} = -2\%$.¹³ For both models, the parameter λ is estimated consistently with Caldeira et al. (2015, p. 74) by minimizing the expression

$$\sum_{t=1}^T \sum_{i=1}^m (\hat{y}_t(\tau_i) - y_t(\tau_i))^2$$

where $y_t(\tau_i) = r_t(\tau_i)$ in the case of the DNS model and $y_t(\tau_i) = \ln(r_t(\tau_i) - r^{min})$ in the case of the Log-DNS model, $\hat{y}_t = r_t - \epsilon_t$, the index t runs from 6.9.2004 to 30.12.2019 and the index i runs through the set of maturities $\{1, 5, 10, 20, 30\}$. Subsequently, the

¹³For a discussion about lower bounds for interest rates, cf. Viñals et al. (2016), who state in the official blog of the International Monetary Fund that “Ballpark estimates by staff for the tipping point at which a move into cash would become worthwhile range from minus 75 basis points (bps) to minus 200 bps”.

parameters $\beta_{1,t}, \beta_{2,t}, \beta_{3,t}$ are estimated per trading day by ordinary least square (OLS) regression.

In the observed time horizon from 2004 to 2019, interest rates have significantly decreased (cf. column “Mean” in Table 1). We remove this drift from the observed Δf_t -processes of both models by deducting the mean of $\Delta f_t^{(i)}$ for each entry i . This helps to avoid the negative drift continuing in the simulated future yield curves. For both models, the lag order p of the VAR-process is chosen according to the criterion of Hannan and Quinn (1979) (HQ).¹⁴ Subsequently, the parameters μ and Γ of the VAR model are estimated by OLS regression per equation. The parameters of the DCC model are estimated with R software using the `rmgarch` package from Ghalanos (2015).¹⁵ According to the Augmented Dickey-Fuller (ADF) test, the disturbances of the VAR-process in Eq. 4 are stationary.

Finally, we estimate the parameters of the ϵ_t -processes for $m = 5$ maturities 1, 5, 10, 20 and 30 years (in line with the maturities of the interest rates published by the ECB). The parameters of the AR(1)-processes for $\epsilon_t(\tau)$ are estimated by OLS regression and the variances of their disturbances are calculated by the unbiased variance estimator. According to the ADF test, these disturbances are stationary.

¹⁴Shittu and Asemota (2009) demonstrate that this criterion outperforms the Akaike information criterion (AIC) and the Bayesian information criterion (BIC) for autoregressive processes and large samples.

¹⁵The estimation works in two steps. In the first step, the parameters $\omega_i, \kappa_i, \lambda_i$ of Eq. 8 are determined by Maximum-Likelihood estimation. Using the predictions for D_t according to Eq. 8, z_t is determined based on Eq. 6. In the second step, a and b of Eq. 9 are estimated.

4 Results and backtesting

4.1 Stochastic interest rate models

We backtest the Value-at-Risks according to the DNS and Log-DNS models by comparing them with losses that would have been realized for the historical yield curve movements. Since the realized loss depends on the composition of the portfolio (which may exhibit long or short exposures for each maturity), the analysis is carried out for 1,000 randomly generated asset-liability portfolios. Each portfolio $i \in \{1, \dots, 1000\}$ consists of two cash inflows at the amount of 2 monetary units and two cash outflows at the amount of 1 monetary unit. The maturities of all cash flows were chosen based on independent random numbers; the calibration of their distribution takes the empirical results of Möhlmann (2020) into account, who has studied the interest rate risk of life insurers based on accounting data. For each inflow, the maturity was chosen using a normal distribution with mean 10 and standard deviation 15; the realization was rounded to a whole number and bounded between 1 and 40. With interest rates per end of 2019, this leads to an average Macaulay duration of cash inflows of 10.0. For comparison, the average asset duration of German life insurers was 10.0 in 2014 and 12.6 in 2018 (cf. Möhlmann, 2020, p. 12). The maturity of each cash outflow was chosen analogously, except for the normal distribution's mean being 15 instead of 10. The average Macaulay duration of cash outflows is 15.0; German life insurers had an average liability duration of 16.9 in 2018 (cf. Möhlmann, 2020, p. 12). The duration gap of the hypothetical insurance companies is 5.4 on average with a standard deviation of 4.4.¹⁶

¹⁶For German life insurers, (Möhlmann, 2020, p. 12) reports an average duration gap of 7.4 (standard deviation: 4.1) in 2014 and 4.3 (standard deviation: 5.9) in 2018.

The Solvency II capital requirement is the 99.5% Value-at-Risk with a 1-year holding period. Backtesting this value with historical data is impossible, since it would require interest rate data from at least 200 years. Instead, we conduct the backtesting for several combinations of holding periods h (in trading days) and confidence levels $1 - \alpha$ and check whether an increase in the holding period h systematically affects the accuracy of the Value-at-Risk estimate.

The backtesting is conducted based on out-of-sample estimates. Hence, when calculating the Value-at-Risk as of day t , we only use data between day 1 and day t to estimate

- the parameters $\lambda, \beta_1, \beta_2, \beta_3$ of Equations 1 and 3,
- the parameters μ, Γ_k of Eq. 4,
- the parameters of the DCC-model (Eq. 8 and 9),
- the parameters of the AR(1) processes for the residuals ϵ_t and
- the standard deviations of the disturbances of the AR(1) processes for ϵ_t .

To determine the Value-at-Risk as of day t over a holding period of h days, we then generate 10,000 simulations of the yield curves r_{t+1}, \dots, r_{t+h} , for both the Log-DNS and the DNS model. The Value-at-Risk for portfolio i , $\text{VaR}_{(1-\alpha),h}^i(t)$, is compared with the historical loss that has occurred for portfolio i between times t and $t + h$:

$$\text{loss}_t^{(i)} = - \sum_{\tau=1}^M (e^{-\tau \cdot r_{t+h}(\tau)} - e^{-\tau \cdot r_t(\tau)}) \cdot CF_{\tau}^{(i)} \quad (25)$$

In order to avoid autocorrelation in the $\text{loss}_t^{(i)}$ -processes, we conduct this comparison only beginning at every h -th day of the observed time period. In line with Caldeira et al.

(2015, p. 73), the backtesting begins at day 500, such that at least 500 days can be used to calibrate the models. We can thereby observe $n = \lfloor \frac{3917-500}{h} \rfloor$ pairwise disjunct time windows, each with a length of h days.

The percentage of days for which the historical loss exceeds the Value-at-Risk is called the hit rate:

$$\text{hit rate} = \frac{1}{n} \sum_t \mathbb{1}_{\{loss_t^{(i)} > VaR_{(1-\alpha),h}^i(t)\}} \quad (26)$$

For an accurate Value-at-Risk estimate for portfolio i , the hit rate should be close to α , i.e. for about $\alpha \cdot n$ days, the historical loss should exceed the Value-at-Risk.

We conduct the analysis for $\alpha = 0.5\%$, $\alpha = 5\%$ and $\alpha = 10\%$ combined with holding periods of $h = 10$, $h = 30$ and $h = 50$ days. These choices have been made in light of Solvency II regulations (for which $\alpha = 0.5\%$ in connection with a holding period of 1 year would be most relevant), calculation time (the smaller h , the larger the number of time windows for which all parameters need to be estimated) and estimate accuracy. The smaller $\alpha \cdot n$ is, the smaller the number of expected hits. For $h = 50$, we obtain only $\lfloor \frac{3917-500}{50} \rfloor = 68$ time windows, meaning that only the hit rate of the 90% Value-at-Risk is relatively meaningful.

The aim of the subsequent analysis is to examine (1) whether a model provides a proper fit in the distribution tail in order to estimate the 99.5% Value-at-Risk, (2) whether a model becomes systematically more optimistic or more conservative when extending the holding period, and (3) whether Value-at-Risk exceedances are clustered in some time periods or occur independently of each other.

To address the first two questions, Table 2 shows the averages and standard deviations of the hit rates across the 1,000 asset-liability portfolios. In addition, we have checked for

each portfolio and each combination of h and α whether the hit rate deviates significantly from the desired level according to Christoffersen's (1998) tests for unconditional coverage. The first part of Table 3 shows the portion of portfolios for which the Value-at-Risk deviates significantly at a 1%, 5% and 10% level of significance.

For the shortest holding period $h = 10$ days, the results in Table 2 suggest that the Log-DNS model provides—on average across all portfolios—suitable estimates for the Value-at-Risk at all three confidence levels. The results in Table 3 confirm that the Value-at-Risk of a large portion of portfolios is not significantly inaccurate. For instance, the hit rate of the 99.5% Value-at-Risk deviates significantly from 0.5% only for 5% of portfolios at a 5% level of significance and for 15% of portfolios at a 10% level of significance. The 95% and 90% Value-at-Risks are suitable even for larger portions of portfolios in this sense. In comparison with the DNS model, the accuracy of the Value-at-Risks provided by the Log-DNS model tends to be better rather than worse. Two conclusions can be drawn from these results: firstly, the Log-DNS model's advantage of respecting a lower bound for interest rates does not come at a disadvantage in terms of the accuracy. Secondly, the Value-at-Risk according to the (Log)-DNS model is suitable not only for an equally-weighted asset portfolio, as demonstrated by Caldeira et al. (2015), but also for various asset-liability portfolios.

Looking at the development of the average hit rates of the 90% and 95% Value-at-Risk when extending the holding period provides little evidence of a systematic change in the accuracy—particularly with regard to the Log-DNS model. Hence, the models appear to be suitable for longer holding periods as well.

Table 2: Averages and standard deviations of hit rates across 1,000 portfolios.

Model	Holding period (in days)	$\alpha = 1 - \text{Confidence level of Value-at-Risk}$					
		0.5%		5%		10%	
		Average	Std Dev.	Average	Std Dev.	Average	Std Dev.
DNS	10	0.43%	0.31%	3.77%	0.52%	8.45%	0.90%
	30	0.19%	0.38%	4.89%	1.30%	7.30%	2.04%
	50	0.68%	0.73%	3.57%	1.19%	8.37%	1.52%
Log-DNS	10	0.67%	0.38%	4.09%	0.56%	8.92%	0.77%
	30	0.30%	0.68%	5.66%	1.44%	8.85%	1.43%
	50	0.09%	0.35%	4.46%	1.58%	8.84%	3.45%

Next, we investigate dependencies of Value-at-Risk exceedances over time. To this end, we employ the independence test of Christoffersen (1998) on the null hypothesis that a Value-at-Risk exceedance does not affect the probability of an exceedance in the subsequent time window. The second part of Table 3 shows the portion of portfolios for which the pattern of Value-at-Risk exceedances is significantly dependent over time.

For the Log-DNS model, the Value-at-Risks exhibit for all considered holding periods, all confidence levels and almost all portfolios no patterns of significantly clustered exceedances. Regarding the DNS model, the exceedances of the 90% Value-at-Risk are dependent at a 10% level of significance for 39% of portfolios when the holding period is 50 days. Again, the Log-DNS model appears to suit for most considered asset-liability portfolios and it tends to perform even better than the DNS model.

Finally, we have applied Christoffersen's (1998) test for conditional coverage, which combines the tests for accuracy (unconditional coverage) and for the independence of Value-at-Risk exceedances. The last part of Table 3 demonstrates that in all considerations, the suitability of the Value-at-Risk according to the Log-DNS model cannot be rejected for at least 92% of portfolios.

Table 3: Portion of portfolios with p-value of Christoffersen’s Exceedance tests below 1%, 5%, and 10%.

Test	Model	Holding period	Confidence level of Value-at-Risk, $1 - \alpha$								
			99.5%			95%			90%		
			p-value below								
			1%	5%	10%	1%	5%	10%	1%	5%	10%
Unconditional coverage	DNS	10	0%	0%	16%	0%	1%	7%	2%	6%	12%
		30	0%	0%	0%	0%	0%	0%	0%	9%	27%
		50	0%	0%	0%	0%	0%	0%	0%	0%	0%
	Log-DNS	10	0%	5%	15%	0%	0%	2%	0%	1%	4%
		30	0%	3%	3%	0%	0%	2%	0%	0%	3%
		50	0%	0%	0%	0%	0%	1%	0%	1%	6%
Independence	DNS	10	0%	0%	0%	0%	10%	13%	1%	6%	13%
		30	0%	0%	0%	0%	0%	0%	0%	1%	1%
		50	0%	0%	0%	0%	3%	7%	0%	6%	39%
	Log-DNS	10	0%	0%	0%	0%	0%	0%	0%	3%	5%
		30	0%	0%	0%	0%	7%	14%	0%	0%	0%
		50	0%	0%	0%	0%	0%	1%	1%	6%	13%
Conditional coverage	DNS	10	0%	0%	0%	0%	6%	14%	2%	9%	16%
		30	0%	0%	0%	0%	0%	0%	0%	6%	11%
		50	0%	0%	0%	0%	0%	3%	0%	3%	7%
	Log-DNS	10	0%	0%	0%	0%	0%	1%	0%	1%	4%
		30	0%	0%	3%	0%	0%	7%	0%	0%	0%
		50	0%	0%	0%	0%	0%	1%	1%	7%	8%

4.2 Scenario-based Value-at-Risk

We now assess how closely the scenario-based approach can reflect the Value-at-Risk of the 1,000 asset-liability portfolios. To this end, we calibrate the Log-DNS model as on 30 December 2019 using the complete time series of yield curve data. We then generate 30,000 simulations for the interest rates $r_{30.12.2019+h}(\tau, \omega)$ for maturities $\tau \in \{1, 5, 10, 20, 30\}$ and time horizons $h \in \{10, 30, 50, 100, 150, 200, 253\}$. 253 is the number of trading days in 2020 and is considered as a 1-year time horizon.

To set up the scenarios, we transform for each h the discount factors according to the simulated interest rates $r_{30.12.2019+h}(\tau, \omega)$ with $\tau \in \{1, 5, 10, 20, 30\}$ into principal components (hence, $m = 5$ in Eq. 14). We then use Eq. 20 and 21 to elicit two stressed interest rates for each of the five modeled maturities and each principal component. Each set of five stressed interest rates is then extrapolated to a complete stressed yield curve by

fitting the Svensson parameters.¹⁷ Finally, the Value-at-Risk is calculated according to Eq. 22.

Table 4 provides the stressed interest rates corresponding to the 99.5% Value-at-Risk over a 1-year holding period for maturities 1, 5, 10, 20 and 30 years. The stressed interest rates are presented in terms of the absolute changes to the interest rates on 30 December 2019. Regarding the first principal component (PC1), the two stress scenarios A and B are essentially an upward and downward shift of interest rates. The second principal component (PC2) governs the steepness of the yield curve by changing long-term interest rates in a different direction than short and middle-term rates. The third principal component (PC3) changes the yield curve at the short end and can, in connection with PC1 and PC2, govern the curvature.

Table 4: Interest rate stress scenarios (in absolute changes to yield curve on 30 December 2019).

		Maturity				
		1 year	5 years	10 years	20 years	30 years
PC1	A	-1.0%	-1.4%	-1.6%	-1.5%	-1.2%
	B	1.1%	1.6%	2.1%	2.5%	2.2%
PC2	A	1.5%	1.0%	0.7%	0.1%	-0.3%
	B	-1.0%	-0.7%	-0.5%	-0.1%	0.1%
PC3	A	1.1%	0.5%	0.0%	-0.2%	0.0%
	B	-1.1%	-0.6%	-0.1%	0.1%	-0.1%

In order to improve the accuracy of the scenario-based Value-at-Risk, we implement correlation parameters (cf. section 2.4). Using the first $\tilde{m} = 2$ principal components, the scenario-based Value-at-Risk is calculated as

$$\widehat{\text{VaR}}(i) = \sqrt{[\text{VaR}_1(i)]^2 + 2 \cdot \rho_{1,2}^{(i)} \cdot \text{VaR}_1(i) \cdot \text{VaR}_2(i) + [\text{VaR}_2(i)]^2} - (\mathbb{E}[X_1] - X_0)^T \cdot S$$

¹⁷For simplicity, $\lambda_{1,t}$ and $\lambda_{2,t}$ are taken from 30.12.2019. Then $\beta_{1,t}, \dots, \beta_{4,t}$ are fitted by OLS.

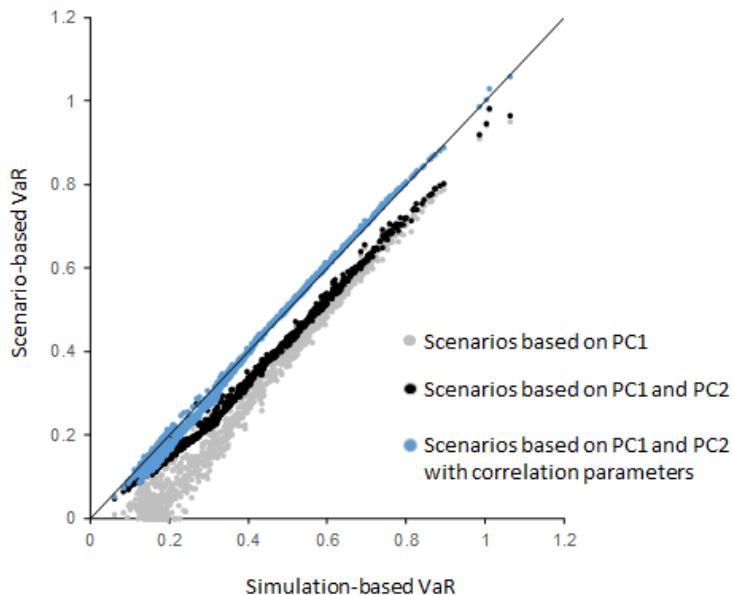
where $\text{VaR}_k(i)$ is the Value-at-Risk of portfolio i relating to the k th principal component, $\rho_{1,2}^{(i)} = \rho_{1,2}^{\text{down}}$ if the downward scenario is relevant to determine $\text{VaR}_1(i)$ and $\rho_{1,2}^{(i)} = \rho_{1,2}^{\text{up}}$ if the upward scenario is relevant to determine $\text{VaR}_1(i)$.¹⁸ In the objective function (cf. line 24), we use the 1,000 portfolios from the backtesting exercises, which are assumed to reflect the regulated insurance companies in the market. The optimal correlation parameters for $h = 253$ are $\rho_{1,2}^{\text{down}} = 0.098$ and $\rho_{1,2}^{\text{up}} = 0.521$. For some holding periods, the optimal correlation parameters may exceed one. For instance, the optimal correlation parameters for $h = 30$ are $\rho_{1,2}^{\text{down}} = 0.283$ and $\rho_{1,2}^{\text{up}} = 1.163$.

We backtest the scenario-based 99.5% Value-at-Risk with all considered holding periods as at year end 2019 by comparing it to the corresponding “exact” Value-at-Risk which is based on the entire simulation. The underlying portfolios are the 1,000 asset-liability portfolios from section 4.1.

Figure 1 depicts the simulation-based Value-at-Risk (x axis) and the scenario-based Value-at-Risk (y axis) for the 1,000 portfolios. The y coordinates of the gray points have been calculated with the two scenarios of PC1 only, those of the black points are based on the four scenarios of PC1 and PC2, and those of the blue points are based on the four scenarios of PC1 and PC2 with outcomes aggregated with optimal correlation parameters. If coordinates of a portfolio lie on the bisector, the scenario-based Value-at-Risk coincides with the simulation-based Value-at-Risk.

¹⁸Differentiating the correlation parameter based on the downward and upward scenario is analogous to the Solvency II standard formula, where the correlation parameter between the the interest rate risk submodule and some other market risk submodules is set in dependence upon which interest rate scenario creates the higher loss.

Figure 1: 99.5% Value-at-Risk over a 1-year holding period as at year end 2019 of 1,000 portfolios according to the entire simulation (x-axis) and scenarios (y-axis).



The results shown in Figure 1 for a 1-year holding period indicate that the scenario-based Value-at-Risk clearly understates the risk when it is determined based only on the two scenarios of PC1. For some portfolios, the scenario-based method would result in a Value-at-Risk close to zero, whereas the Value-at-Risk based on the entire simulation suggests a substantial risk. Those scenarios might represent portfolios which are immunized by duration matching against yield curve shifts, but not against changes in the yield curve's steepness or curvature. Calculating the Value-at-Risk based on the four scenarios of PC1 and PC2 and using correlation parameters substantially improves the accordance of the scenario-based with the simulation-based Value-at-Risk.

Table 5 shows the backtesting results for all considered holding periods and three versions of the scenario-based Value-at-Risk (PC1 only, PC1 and PC2 without and with correlation

Table 5: Average simulation-based Value-at-Risk and root mean squared error (RMSE) of scenario-based Value-at-Risk in comparison to simulation-based Value-at-Risk across 1,000 portfolios. Percentages compare RMSE against those of PC1.

Holding period h	Average VaR	RMSE without correlations			RMSE with correlations	
		PC1	PC1 and PC2		PC1-PC2	
10	0.0380	0.0110	0.0086	-21.8%	0.0074	-32.7%
30	0.0722	0.0188	0.0149	-20.8%	0.0127	-32.4%
50	0.0962	0.0240	0.0186	-22.7%	0.0152	-36.5%
100	0.1609	0.0429	0.0331	-23.0%	0.0213	-50.4%
150	0.2180	0.0583	0.0419	-28.1%	0.0245	-58.0%
200	0.2912	0.0776	0.0570	-26.5%	0.0244	-68.5%
253	0.3691	0.1127	0.0518	-54.1%	0.0104	-90.8%

parameters). The measurement error of the scenario-based Value-at-Risk is determined by the root mean squared error (RMSE), which is calculated as

$$\sqrt{\sum_{i=1}^{1000} \left(\widehat{\text{VaR}}(i) - \text{VaR}(i) \right)^2} \quad (27)$$

where $\text{VaR}(i)$ denotes the simulation-based Value-at-Risk and $\widehat{\text{VaR}}(i)$ denotes the scenario-based Value-at-Risk of portfolio i . The inclusion of correlation parameters improves the accuracy of the scenario-based Value-at-Risk specifically for long holding periods. This is because the stochastic dependencies between the discount factors of different maturities become increasingly nonlinear as the length of the holding period h grows. Figure 2 demonstrates that the simulated discount factors after $h = 10$ days for different maturities can be well described by linear dependencies. After one year, in contrast, there is a non-linear curved relationship between the discount factors. The PCA, by construction, builds on a spectral decomposition of the covariance matrix. Hence, it can only account for linear relationships.

Finally, Figure 3 sets the RMSE of the scenario-based VaR according to PC1 and PC2 in relation to the corresponding simulation-based VaR (on average across the 1,000 portfolios). In relative terms, the error of the scenario-based VaR with correlation parameters

(blue points) clearly decreases as the holding period increases. This indicates that the essential yield curve movements of the chosen stochastic model are, in the long run, well described by the first two principal components. Regarding the scenario-based VaR without correlation parameters (black points), the relative error tends to decrease in the holding period. Here, the downward trend is not so clear due to the increasing non-linearity effects as illustrated in Figure 2.

Figure 2: Simulated discount factors after $h = 10$ days and $h = 254$ days (1 year).

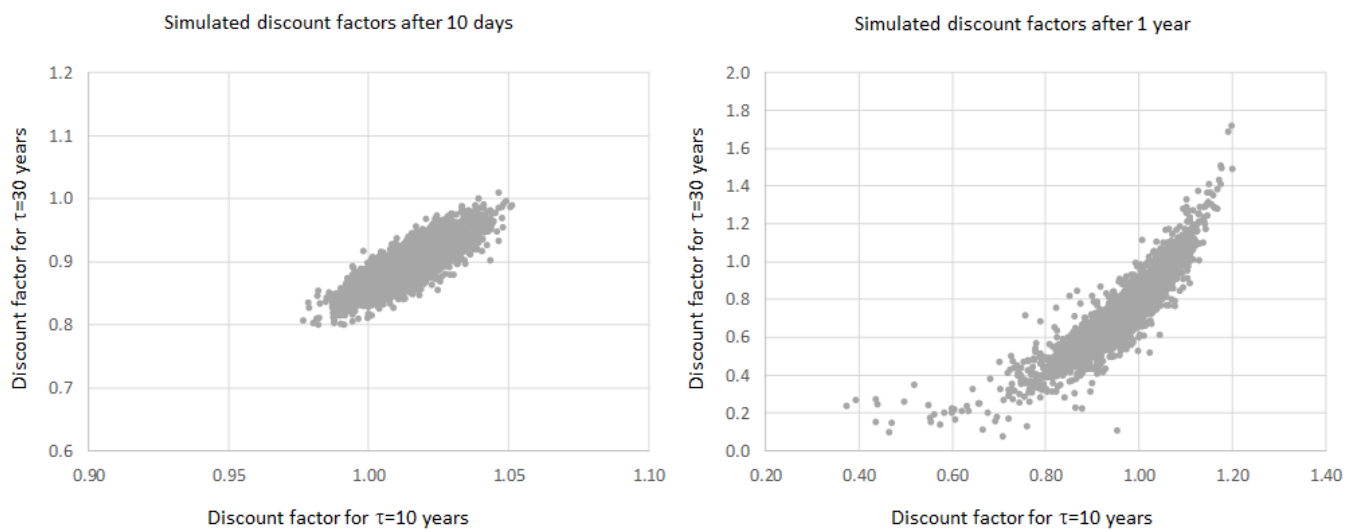
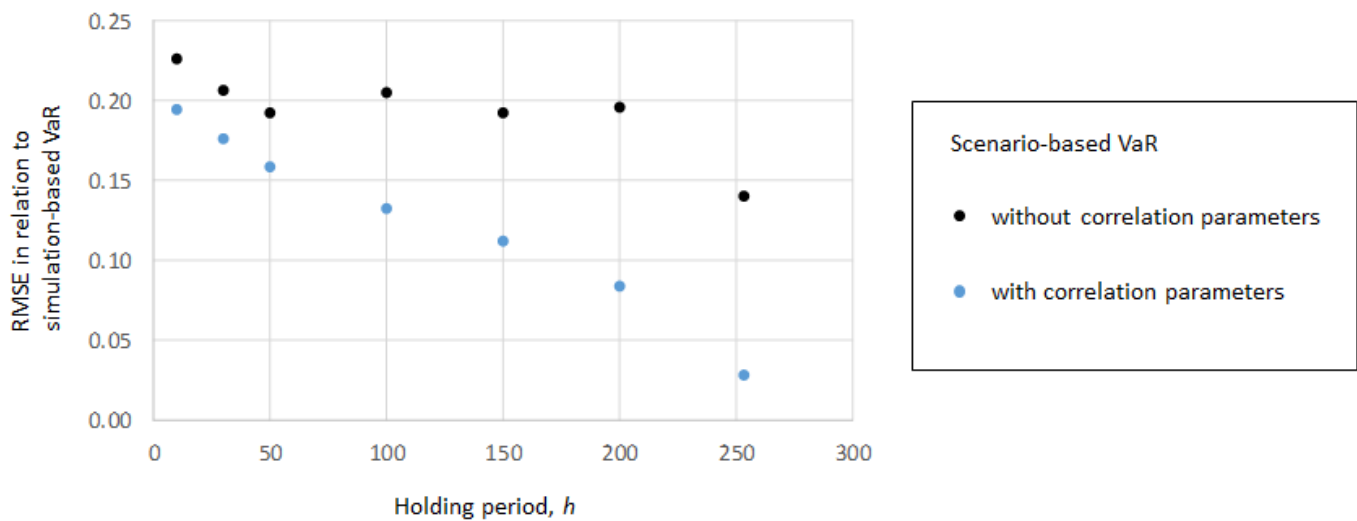


Figure 3: Root mean squared error (RMSE) of scenario-based Value-at-Risk divided by the average simulation-based Value-at-Risk. Scenario-based Value-at-Risk is calculated based on PC1 and PC2 with and without correlation parameters.



5 Conclusion

This paper demonstrates how a scenario-based VaR can be derived based on a PCA from yield curve simulations. The simulations are derived from the dynamic version of the Nelson-Siegel model which can be modified such that interest rates have a lower bound. Our analytical derivation of the scenario-based VaR points out that the PCA needs to be applied to the discount factors (not to the yield curves themselves). Given that the discount factors do not follow an elliptical distribution—especially for long time horizons, their stochastic interdependencies are not linear—non-zero correlation parameters in the aggregation of the scenario outcomes can substantially improve the suitability of the scenario-based VaR.

References

- Bank for International Settlements, 2016. Basel Committee on Banking Supervision. Interest rate risk in the banking book. URL: <http://www.bis.org/bcbs/publ/d368.pdf>.
- Braun, A., Schmeiser, H., Schreiber, F., 2017. Portfolio optimization under Solvency II: Implicit constraints imposed by the market risk standard formula. *Journal of Risk and Insurance* 84, 177–207.
- Caldeira, J., Moura, G., Santos, A., 2015. Measuring risk in fixed income portfolios using yield curve models. *Computational Economics* 46, 65–82.
- Campbell, R., Koedijk, K., Kofman, P., 2002. Increased correlation in bear markets. *Financial Analysts Journal* 58, 87–94.
- Christoffersen, P.F., 1998. Evaluating interval forecasts. *International Economic Review* 39, 841–862.
- Committee of European Insurance and Occupational Pensions Supervisors (CEIOPS), 2010. Solvency II calibration paper, CEIOPS-SEC-40-10.
- Cox, J.C., Ingersoll Jr, J.E., Ross, S.A., 1985. A theory of the term structure of interest rates. *Econometrica* 53, 385–407.
- Diebold, F.X., Li, C., 2006. Forecasting the term structure of government bond yields. *Journal of Econometrics* 130, 337–364.
- Duffee, G.R., 2002. Term premia and interest rate forecasts in affine models. *Journal of Finance* 57, 405–443.

- Eder, A., Keiler, S., Pichl, H., 2014. Interest rate risk and the Swiss Solvency Test. *European Actuarial Journal* 4, 77–99.
- Engle, R., 2002. Dynamic conditional correlation: a simple class of multivariate generalized autoregressive conditional heteroskedasticity models. *Journal of Business & Economic Statistics* 20, 339–350.
- European Commission, 2015. Commission Delegated Regulation (EU) 2015/35 of 10 October 2014 supplementing Directive 2009/138/EC of the European Parliament and of the Council on the taking-up and pursuit of the business of Insurance and Reinsurance (Solvency II).
- European Insurance and Occupational Pensions Authority (EIOPA), 2019. Consultation paper on the opinion on the 2020 review of Solvency II.
- Fischer, K., Schlütter, S., 2014. Optimal investment strategies for insurance companies when capital requirements are imposed by a standard formula. *Geneva Risk and Insurance Review* 40, 15–40.
- Frye, J., 1997. Principals of risk: Finding var through factor-based interest rate scenarios, in: *VAR: Understanding and Applying Value at Risk*. Risk Publications, London, pp. 275–288.
- Fung, D.W., Jou, D., Shao, A.J., Yeh, J.J., 2018. The China Risk-Oriented Solvency System: a comparative assessment with other risk-based supervisory frameworks. *The Geneva Papers on Risk and Insurance—Issues and Practice* 43, 16–36.

- Gatzert, N., Martin, M., 2012. Quantifying credit and market risk under Solvency II: Standard approach versus internal model. *Insurance: Mathematics and Economics* 51, 649–666.
- Gerstner, T., Griebel, M., Holtz, M., Goschnick, R., Haep, M., 2008. A general asset–liability management model for the efficient simulation of portfolios of life insurance policies. *Insurance: Mathematics and Economics* 42, 704–716.
- Ghalanos, A., 2015. rmgarch: Multivariate garch models. r package version 1.3-0 .
- Golub, B.W., Tilman, L.M., 1997. Measuring yield curve risk using principal components analysis, value at risk, and key rate durations. *Journal of Portfolio Management* 23, 72.
- Graf, S., Kling, A., Ruß, J., 2011. Risk analysis and valuation of life insurance contracts: Combining actuarial and financial approaches. *Insurance: Mathematics and Economics* 49, 115–125.
- Hannan, E., Quinn, B., 1979. The determination of the order of an autoregression. *Journal of the Royal Statistical Society, Series B* 41, 190–195.
- Hull, J.C., 2018. *Options, Futures and other Derivatives*, 9th Edition.
- International Association of Insurance Supervisors (IAIS), 2020. Level 2 Document: ICS Version 2.0 for the monitoring period.
- Laas, D., Siegel, C.F., 2017. Basel III versus Solvency II: An analysis of regulatory consistency under the New Capital Standards. *Journal of Risk and Insurance* 84, 1231–1267.

- Martin, M., 2013. Assessing the model risk with respect to the interest rate term structure under Solvency II. *The Journal of Risk Finance* 14, 200–233.
- McNeil, A.J., Frey, R., Embrechts, P., 2015. *Quantitative Risk Management: Concepts, Techniques and Tools - Revised Edition*. Princeton Series in Finance.
- Mittnik, S., 2014. Var-implied tail-correlation matrices. *Economics Letters* 122, 69–73.
- Möhlmann, A., 2020. Interest rate risk of life insurers: Evidence from accounting data. *Financial Management*, 1–26.
- Nelson, C.R.N., Siegel, A.F., 1987. Parsimonious modeling of yield curves. *The Journal of Business* 60, 473–489.
- Shittu, O., Asemota, M., 2009. Comparison of criteria for estimating the order of autoregressive process: A Monte Carlo approach. *European Journal of Scientific Research* 30, 409–416.
- Svensson, L.E.O., 1994. Estimating and interpreting forward interest rates: Sweden 1992-1994. IMF Working Papers 94/114.
- Vasicek, O., 1977. An equilibrium characterization of the term structure. *Journal of Financial Economics* 5, 177–188.
- Vedani, J., Karoui, N.E., Loisel, S., Prigent, J.L., 2017. Market inconsistencies of market-consistent European life insurance economic valuations: pitfalls and practical solutions. *European Actuarial Journal* 7, 1–28.
- Viñals, J., Gray, S., Eckhold, K., 2016. The broader view: The positive effects of negative nominal interest rates. URL:

<https://blogs.imf.org/2016/04/10/the-broader-view-the-positive-effects-of-negative-nominal-interest-rates>.